

Galaxy triplets in SDSS-DR7: I. Catalogue

Ana Laura O’Mill^{3*}, Fernanda Duplancic^{4,2}, Diego García Lambas^{1,2}, Carlos Valotto^{1,2} & Laerte Sodré Jr³

¹ Instituto de Astronomía Teórica y Experimental, IATE, Observatorio Astronómico, Universidad Nacional de Córdoba, Laprida 854, X5000BGR, Córdoba Argentina

² Consejo de Investigaciones Científicas y Técnicas (CONICET), Avenida Rivadavia 1917, C1033AAJ, Buenos Aires, Argentina

³ Departamento de Astronomia, Instituto de Astronomia, Geofísica e Ciências Atmosféricas da USP, Rua do Matão 1226, Cidade Universitária, 05508-090, São Paulo, Brazil.

⁴ Instituto de Ciencias Astronómicas, de la Tierra y del Espacio, ICATE, Casilla de Correo 49, CP 5400, San Juan, Argentina.

8 November 2018

ABSTRACT

We present a new catalogue of galaxy triplets derived from the Sloan Digital Sky Survey Data Release 7. The identification of systems was performed considering galaxies brighter than $M_r = -20.5$ and imposing constraints over the projected distances, radial velocity differences of neighbouring galaxies and isolation. To improve the identification of triplets we employed a data pixelization scheme, which allows to handle large amounts of data as in the SDSS photometric survey. Using spectroscopic and photometric data in the redshift range $0.01 \leq z \leq 0.40$ we obtain 5901 triplet candidates. We have used a mock catalogue to analyse the completeness and contamination of our methods. The results show a high level of completeness ($\sim 80\%$) and low contamination ($\sim 5\%$). By using photometric and spectroscopic data we have also addressed the effects of fiber collisions in the spectroscopic sample. We have defined an isolation criterion considering the distance of the triplet brightest galaxy to closest neighbour cluster, to describe a global environment, as well as the galaxies within a fixed aperture, around the triplet brightest galaxy, to measure the local environment. The final catalogue comprises 1092 isolated triplets of galaxies in the redshift range $0.01 \leq z \leq 0.40$. Our results show that photometric redshifts provide very useful information, allowing to complete the sample of nearby systems whose detection is affected by fiber collisions, as well as extending the detection of triplets to large distances, where spectroscopic redshifts are not available.

Key words: Galaxies: systems: general

1 INTRODUCTION

In a hierarchical scenario, the interactions affects general properties of the galaxies such as star formation rate, nuclear activity and morphology (Alonso et al. 2004, 2006)

Although galaxy pairs (Lambas et al. 2003; Alonso et al. 2004, 2006) and groups with four or more members (Merchán & Zandivarez 2005) have been the subject of several papers in the literature, there are far few works on triplets of galaxies, a link between pairs and groups and a potentially interesting laboratory to investigate several process associated to galaxy evolution.

Traditionally, galaxy groups selection have excluded triplets of galaxies because these systems were not considered as bonafide physical structures, i.e., dynamically isolated systems. Neverthe-

less, Hernández-Toledo et al. (2011) have recently analysed a sample of galaxy triplets derived from the catalogue of isolated triplets of Karachentseva (1973) finding signatures of physical interactions (tidal bridges, excess of barred galaxies), that implies that most of these objects are indeed real physical structures.

Pioneering works on the identification of triplets of galaxies were performed by Karachentseva et al. (1979) and Karachentsev et al. (1988). These authors present a list of 84 Northern isolated galaxy triplets with members with component apparent magnitudes brighter than 15.7, selected by visual inspection of Palomar Sky Survey prints. They found that about 24% of the members are elliptical and lenticular galaxies, while 76% are spirals and irregulars. Numerous studies have been made in the follow up of this catalogue. Karachentsev & Karachentseva (1981) measured radial velocities for the isolated triplets and found that 5% of the systems are spurious ($\Delta V_{ij} > 500 \text{ km s}^{-1}$), 31% consist of a pair of galaxies with nearly equal radial ve-

* E-mail: aomill@oac.uncor.edu

locities ($\Delta V_{ij} < 500 \text{ km s}^{-1}$) and a projected third component and 64% are considered physical triplets ($\Delta V_{ij} < 500 \text{ km s}^{-1}$). Velocity dispersion, diameters, integrated luminosity, virial mass, and the virial mass to luminosity ratio were estimated for the physical triplets (Karachentseva & Karachentsev 1982, 1983). The spatial configuration, dynamics and dark matter content of these systems was studied by several authors (Karachentsev et al. 1990; Chernin & Mikkola 1991; Anosova et al. 1992; Zheng et al. 1993; Aceves 2000). For the Southern sky ($\delta < -3^\circ$) Karachentseva & Karachentsev (2000) selected 76 isolated triple systems of galaxies using the ESO/SERC and POSS-I sky surveys, with the same criteria defined for the Northern systems.

Trofimov & Chernin (1995) compiled a list of 108 triplets of galaxies selected from two group catalogues, those of Geller & Huchra (1983) (Northern sky) and Maia et al. (1989) (Southern sky). 38 of these systems are considered isolated. The authors call these systems “wide triplets” in contrast to the compact triplets (with smaller mean projected harmonic separation) studied by Karachentseva et al. (1979). The main assumed difference between wide and compact systems, regardless their difference in size, is that galaxies in compact triplets are supposed to have interacted many times and are probably in equilibrium within the system. In contrast, wide triplets would be dynamically young and probably far from virialization.

A high-order 3D Voronoi tessellation method was employed by Elyiv et al. (2009) for identifying single galaxies, pairs and triplets on a volume-limited sample of galaxies from the Sloan Digital Sky Survey Data Release 5. Nevertheless, a catalogue of triplet of galaxies has not been compiled for more recent SDSS releases.

In this work we present a catalogue of triplets of bright galaxies ($M_r < -20.5$) selected from a volume limited sample extracted from SDSS-DR7 in the redshift range $0.01 \leq z \leq 0.4$. We used data with both spectroscopic redshift measurements and photometric redshifts from O’Mill et al. (2011).

This paper is organized as follows. In Section 2 we describe the galaxy samples used in this work. Section 3 describes the algorithm developed for the detection of triplet of galaxies candidates. The implementation of this algorithm at low redshifts is described in Section 4. In this section we also perform a completeness and contamination test to our algorithm and analyse the incompleteness effect due to fiber collisions. Section 5 describes the extension of our results to higher redshifts. In Section 6 we describe the isolation criteria employed to define the final sample of triplet of galaxies. Finally, Section 7 summarized the results obtained in this work.

Throughout this paper we adopt a cosmological model characterised by the parameters $\Omega_m = 0.25$, $\Omega_\Lambda = 0.75$ and $H_0 = 70 \text{ km s}^{-1} \text{ Mpc}^{-1}$.

2 SPECTROSCOPIC AND PHOTOMETRIC GALAXY SAMPLES

The samples of galaxies used in this work were drawn from the Data Release 7 of Sloan Digital Sky Survey (SDSS-DR7, Abazajian et al. 2009). SDSS (York et al. 2000) has mapped more than one-quarter of the entire sky, performing photometry and spectroscopy for galaxies, quasars and stars. SDSS-DR7 is the seventh major data release, corresponding to the completion of the survey SDSS-II. It comprises 11.663 sq. deg. of imaging data, with an increment of ~ 2000 sq. deg., over the previous data release, mostly in regions of low Galactic latitude. SDSS-DR7 provides imaging data for 357 million distinct objects in five bands, *ugriz*,

as well as spectroscopy over $\simeq \pi$ steradians in the North Galactic cap and 250 square degrees in the South Galactic cap. The average wavelengths corresponding to the five broad bands are 3551, 4686, 6165, 7481, and 8931 Å (Fukugita et al. 1996; Hogg et al. 2001; Smith et al. 2002). For details regarding the SDSS camera see Gunn et al. (1998); for astrometric calibrations see Pier et al. (2003). The survey has spectroscopy over 9380 sq. deg.; the spectroscopy is now complete over a large contiguous area of the Northern Galactic Cap, closing the gap that was present in previous data releases.

In this work we employed spectroscopic and photometric data extracted from SDSS-DR7. The spectroscopic data were derived from the Main Galaxy Sample (MGS; Strauss et al. (2002)) obtained from the `fits` files at the SDSS home page¹. `k`-corrections for this sample were calculated using the software `k-correct_v4.2` of Blanton & Roweis (2007). The photometric data were derived from the photometric catalogue constructed by O’Mill et al. (2011)². These authors compute photometric redshift and `k`-correction for the photometric data of the SDSS-DR7. The *rms* of the photometric redshift is $\sigma_{phot} \sim 0.0227$ and `k`-corrections were obtained through joint parametrisation of redshift and reference frame (at $z = 0.1$) ($g - r$) colour. For both data sets, `k`-corrected absolute magnitudes were calculated from Petrosian apparent magnitudes converted to the AB system.

In order to use these spectroscopic and photometric data, it is necessary to analyse the completeness and reliability of these samples. To explore this issue we have calculated the spatial number density of galaxies brighter than $M_r = -20.5$ for both spectroscopic and photometric data, taking into account the apparent magnitude limit $r = 17.77$ and $r = 21.5$, respectively. In Figure 1 it can be appreciated that the spatial number density of galaxy for, both, spectroscopic and photometric samples, shows a flat trend up to $z \sim 0.14$ and $z \sim 0.4$ respectively. The spatial number density of galaxies for the photometric data shown in Figure 1 corresponds to a random sample with $\sim 0.001\%$ of the complete photometric sample.

Taking into account these considerations we derived four galaxy data sets from SDSS-DR7:

The first sample, hereafter S1, comprises galaxies brighter than $r = 17.77$ with spectroscopic redshift in the range $0.01 \leq z_{spec} < 0.14$. This sample was employed for the detection of triple systems of galaxies candidates at low redshift.

In order to analyse the effect of photometric errors over the radial velocity differences ΔV for the photometric data, we have selected a sample that comprises galaxies brighter than $r = 17.77$ with spectroscopic measurements in the redshift range $0.07 \leq z_{spec} \leq 0.12$ for which we have obtained photometric redshifts. We will refer to this sample hereafter as the S2 sample.

We have also extracted a sample of galaxies brighter than $r = 17.77$, that comprises galaxies with spectroscopic measurements in the redshift range $0.09 \leq z_{spec} \leq 0.11$ and galaxies with photometric redshifts in the range $0.09 - \sigma_{phot} \leq z_{phot} \leq 0.11 + \sigma_{phot}$ (hereafter S3). This sample was employed in the analysis of completeness due to fiber collision, described in Section 4.

Finally, for the detection of triplets of galaxies candidates at intermediate redshift we employed a sample derived from the photometric catalogue of O’Mill et al. (2011). We have selected a sample that comprises galaxies brighter than $r = 21.5$, in the redshift

¹ <http://www.sdss.org/dr7/products/spectra/getspectra.html>

² Available at <http://casjobs.starlight.ufsc.br/casjobs>

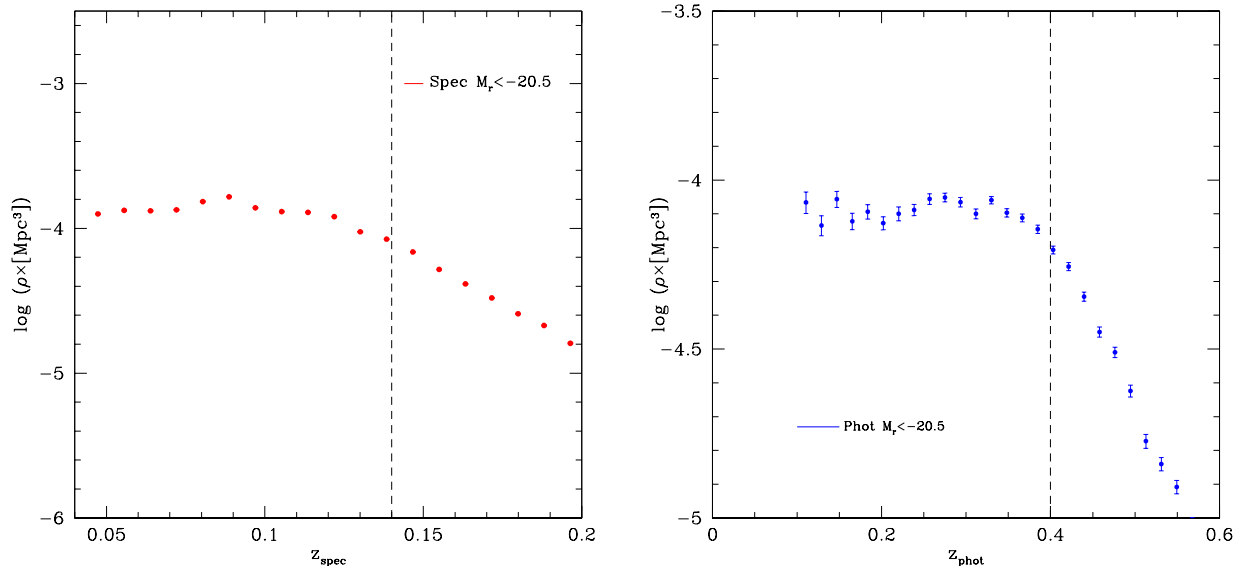


Figure 1. Spatial number density of galaxies brighter than $M_r = -20.5$. *Left:* Spectroscopic data with apparent magnitude $r < 17.77$. *Right:* Random sample of $\sim 0.001\%$ of the photometric sample with apparent magnitude $r < 21.5$. Error bars represent 1σ uncertainties calculated by bootstrap. The vertical line shows the limits chosen for the detection of the triple candidate systems.

range $0.09 \leq z_{\text{phot}} \leq 0.5$. We will refer to this sample as S4 hereafter.

Table 1 summarises the main characteristics of the different samples used in this work.

3 BUILDING THE CATALOGUE

In this section we present the algorithm adopted to identify galaxy triplet candidates from the spectroscopic and photometric volume limited samples of SDSS-DR7. The algorithm searches for triplets by selecting galaxies within a given projected distance (r_p) and radial velocity difference (ΔV) of another galaxy.

Lambas et al. (2003) identified pairs of galaxies using $r_p = 100 h^{-1}$ kpc and $\Delta V = 350 \text{ km s}^{-1}$. Merchán & Zandivarez (2005) identified galaxy groups in the SDSS third data release with a mean redshift of 0.1 and a median velocity dispersion of 230 km s^{-1} . These authors employed a fiends-of-friends algorithm with a transverse linking length corresponding to an overdensity of 80 and a line-of-sight linking length of $\Delta V = 200 \text{ km s}^{-1}$. For the detection of triple galaxy systems, we have considered these restrictions in the selection of r_p and ΔV constrains.

3.1 Data Pixelization

For the purpose of a suitable selection of the systems, as well as to efficiently reduce the computing time, we have used a pixelization of SDSS data. Indeed, data pixelization is an important tool in managing large amounts of information such as that contained in the SDSS photometric catalogue.

In order to perform a pixelization of SDSS data, we have employed routines of the Hierarchical Equal Area Pixelization iso-Latitude software (HEALPIX, Górski et al. 2005). HEALPIX was developed for data processing and analysis of the observations of

the cosmic microwave background (CMB). This pixelization procedure consists in an equal area isolatitude partition of the sphere, which results into a versatile structure for data analysis. The resolution base comprises 12 pixels formed by three rings around the poles and the equator. For higher resolutions, each pixel is subdivided into four equal-area pixels of smaller size. The grid resolution is set by the N_{side} parameter, which defines the number of divisions along the side of a pixel, required to achieve the high-resolution partition desired. All pixel centres are equidistant in azimuth for each ring and are placed on rings of constant latitude. All rings located in the equatorial zone are divided in the same number of pixels, $N_{\text{eq}} = 4N_{\text{side}}$. The rings located in the polar cap region contain a varying number of pixels that increase by one pixel within each quadrant, with increasing distance from the poles. The resulting map contains $N_{\text{pix}} = 12N_{\text{side}}^2$ pixels of equal area $A = \pi/N_{\text{side}}^2$.

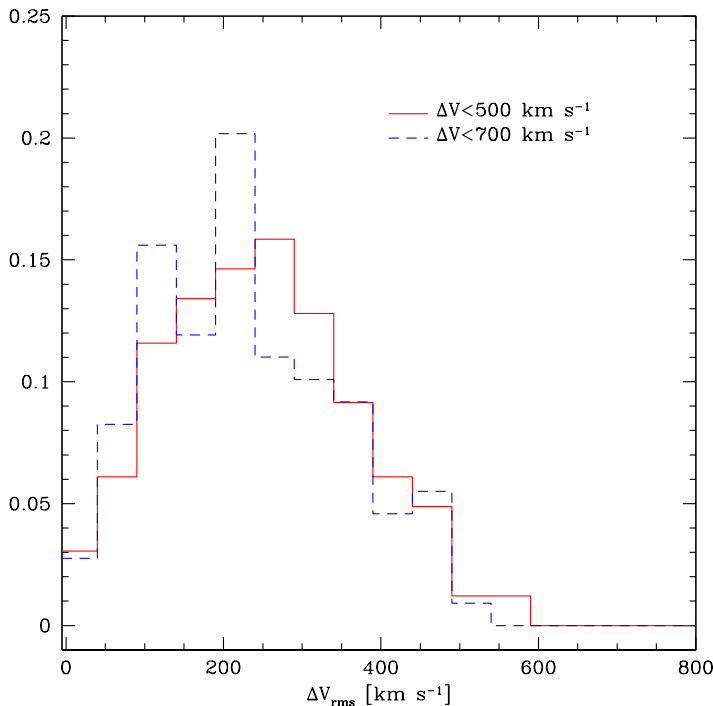
HEALPIX has a library of computational algorithms and visualisation software that allows fast scientific applications on discretized maps created from large amounts of data as is the SDSS survey.

We have employed HEALPIX routines to find the index of all pixels within a radial angular distance from a defined center. The routines used were: *ang2pix*, which generates a linking list for galaxies in each pixel; *ang2vec*, that converts angular to Cartesian coordinates, and, finally, *query_disc*, that identifies the central galaxy pixel and the adjacent pixels inside the search radius, previously defined. The resolution (N_{side}) was set to 512 at redshift smaller than 0.14 (S1, S2 and S3 samples) and 2048 at redshift greater than 0.14 (S4 sample). The choice of different values of N_{side} is due to the density difference between the lower and intermediate redshift samples.

For each selected center we define a search radius that covers approximately $600 h^{-1}$ kpc at the smallest redshift of each sample, ensuring the search in every pixel adjacent to the center. The

Table 1. Description of the samples used in this work.

sample name	Description	number of objects
S1	MGS spectroscopic data. Used for the identification of triplets of galaxies candidates at low redshift ($0.01 \leq z_{\text{spec}} < 0.14$)	684939
S2	MGS with photometric redshift ($0.07 \leq z_{\text{spec}} \leq 0.12$). Used in section 4.3	248210
S3	MGS and photometric data. Used in the fiber collision analysis	80851 and 860021
S4	Photometric catalogue with redshifts and k-correction from O’Mill et al. (2011) Used for the identification of triplets of galaxies candidates at intermediate redshift ($0.09 \leq z_{\text{phot}} \leq 0.5$)	66390174

**Figure 2.** Distribution of ΔV_{rms} for triplet candidates identified in the spectroscopic sample S1. Red (continuous) line: $r_p < 100 h^{-1}$ kpc and $\Delta V < 500 \text{ km s}^{-1}$. Blue (dashed) line: systems with $r_p < 200 h^{-1}$ kpc and $\Delta V < 700 \text{ km s}^{-1}$.

adopted search radii were: 0.88 deg for S1, S2 and S3 samples and 0.068 deg for the S4 sample.

3.2 The algorithm

In this section we describe the successive steps of the algorithm developed for the identification of triplet of galaxies candidates.

Step 1: The algorithm begins with a selection of central galaxy candidates. The pixel of each candidate is identified. Then a search for galaxies belonging to adjacent pixels, enclosed within the search radius, is performed. In the first run, any galaxy is considered a central galaxy candidate.

Step 2: To identify triplet systems, we have considered as neighbours all those galaxies that satisfy the constraints in pro-

jected distance and radial velocity difference, ie. $r_p < r_{pmax}$ and $\Delta V < \Delta V_{max}$.

Step 3: We consider a triplet candidate when there are only three galaxies within the constraints in Step 2.

Step 4: Then, we assign the brightest galaxy to the center of each system. This generate two types of multiple identifications:

- The center is assigned to more than one system independently identified. This is because the brightest galaxy is a neighbour galaxy in more than one system.
- A system will be identified more than once if different centres satisfy the neighbourhood condition, ie have $r_p < r_{pmax}$ and $\Delta V < \Delta V_{max}$.

In order to avoid double identifications, repeated centres were removed from the sample and close galaxy pair centres were considered as a single system by taking the brightest galaxy as a central

galaxy. This procedure generates a new sample of central galaxies. With these centres as input sample, the algorithm returns to Step 1.

Step 5: It may happen that the new central galaxies may be located at a distance greater than r_{pmax} or have a radial velocity difference greater than ΔV_{max} with respect to one of the selected neighbours. To retrieve these systems, we consider a second set of constraints, relaxing restrictions over velocity difference and projected distance, and then returning to Step 2.

4 IMPLEMENTATION OF THE ALGORITHM AT LOW REDSHIFT ($0.01 \leq z_{spec} < 0.14$)

The aim of this work is the identification of triplets of luminous galaxies, defined as systems close in projected distance and radial velocities. Building of a catalogue of triplets with spectroscopic measurements is less subject to contamination than using photometric redshifts given the small uncertainties. So, in principle, using spectroscopic data results into a more reliable identification of these objects.

4.1 Spectroscopic data

In order to identify triplets of galaxies candidates in the S1 sample, we have run the algorithm considering the following restrictions for the selection of neighbouring galaxies: $r_p < 100 h^{-1}$ kpc and $\Delta V < 500 \text{ km s}^{-1}$.

Following the steps described in the previous section, we have assigned the center to the brightest galaxy of the system. After this recentering, we have considered a second group of constraints $r_p < 200 h^{-1}$ kpc and $\Delta V < 700 \text{ km s}^{-1}$, in order to retrieve the systems lost by the procedure.

Therefore, a total of 273 triple system candidates were obtained from the S1 sample, 164 of them with the constraints $r_p < 100 h^{-1}$ kpc and $\Delta V < 500 \text{ km s}^{-1}$ and 109 with $r_p < 200 h^{-1}$ kpc and $\Delta V < 700 \text{ km s}^{-1}$.

Figure 2 shows the distribution of ΔV_{rms} , where ΔV_{rms} is the root mean square radial velocity difference for the systems. Red lines correspond to the triplet candidates obtained with $r_p < 100 h^{-1}$ kpc and $\Delta V < 500 \text{ km s}^{-1}$ and in blue lines we present the systems obtained with $r_p < 200 h^{-1}$ kpc and $\Delta V < 700 \text{ km s}^{-1}$. Both distributions present a similar behaviour.

4.2 Completeness and contamination tests

In order to test the algorithms, we performed a completeness and contamination test employing a SDSS mock catalogue derived from the semi-analytic models of Croton et al. (2006), obtained from the Millennium Simulation (Springel et al. 2005) outputs. The spatial resolution of this simulation is suitable for the implementation of our algorithm. The luminosity function of the semi-analytic model is consistent with observations of galaxies at low redshift. The mock catalogue comprise 514914 galaxies brighter than $r = 17.77$, where r correspond to the r -band magnitude of the SDSS. This mock catalogue contains: right ascension, declination, apparent magnitude in r -band, halo mass, redshift and peculiar velocity.

For the completeness and contamination test we have employed a volume limited mock catalogue considering galaxies brighter than $M_r = -20.5$ in the redshift range $0.01 \leq z < 0.14$.

The completeness is defined as N_{rec}/N_{tot} , where N_{rec} is the number of triplet candidates identified with our algorithm that are

matched to the systems found in real space (recovered triplets), and N_{tot} is the number of systems selected with real distances (real triplets)³ within the same halo. We find that the completeness achieved by our algorithm is $\sim 80\%$.

The contamination is defined as N_{sp}/N_{det} , where N_{det} is the number of triplet candidates identified with r_p and ΔV . N_{sp} is number of systems detected whose member galaxies do not belong to the same halo (spurious triplets). The contamination for our triplet sample is very small, $\sim 5\%$.

Figure 3 shows the redshift distribution for the real, recovered and spurious triplet of galaxies, as well as the dependence of the completeness and contamination rates with redshift.

4.3 Analysis of photometric data in the spectroscopic redshift range

The major source of contamination in the detection of the photometric systems is due to the error in z_{phot} , since the uncertainties in photometric redshifts affects the choice of ΔV . To evaluate this point, we employed the S2 sample. We have run the algorithm for different values of ΔV , corresponding to $1\sigma_{phot} * c$, $1.5\sigma_{phot} * c$ and $2\sigma_{phot} * c$, where σ_{phot} is the mean photometric redshift error ($\sigma_{phot} \sim 0.0227$, as previously mentioned in Section 2) and c is the speed of light. We have then examined the distribution of the values of the *rms* spectroscopic velocity differences $\sigma_{\Delta V}$, considering the spectroscopic redshifts of the triplet candidate members identified photometrically.

For the S2 sample we identified 80 triplet candidates that satisfy the constraints described in section 4.1. Using photometric data we recover 71 of these systems considering $1\sigma_{phot}$ and $1.5\sigma_{phot}$ for ΔV . For $2\sigma_{phot}$ we recovered all the spectroscopic triplets.

In figure 4 we show the $\sigma_{\Delta V}$ distribution of triplet candidates identified in S2 sample. In different lines and colours we show the systems identified with $1\sigma_{phot}$ in red, $1.5\sigma_{phot}$ in magenta, and $2\sigma_{phot}$ in blue line. From the figure it can be appreciated that we have a large level of contamination when using $1.5\sigma_{phot}$ and $2\sigma_{phot}$. Therefore, we conclude that the $1\sigma_{phot}$ interval provides a suitable compromise between high completeness and low contamination.

4.4 Incompleteness due to fiber collisions

The SDSS spectrograph uses fibers manually connected to plates in the telescope's focal plane. These fibers are mapped through a mosaic algorithm (Blanton et al. 2003) that optimises the observation of large-scale structures. Two fibers can not be placed closer than $55''$ (Strauss et al. 2002), so for two objects with the same priority (such as two MGS galaxies) and whose centres are closer than $55''$, the algorithm selects at random the galaxy which will be observed spectroscopically. There are regions where the plates overlap (about 30% of the mosaic regions), in which both objects may be observed.

Due to fiber collision the spectroscopic sample is affected by incompleteness. The magnitude limit of spectroscopic objects is $r = 17.77$, but not all galaxies brighter than this limit were observed. This issue becomes more important when analysing compact objects.

³ $r_p = r \times \cos(\theta) \times d\theta \times d\Phi$, where r , θ and Φ are the spherical coordinates with origin in the triplets center.

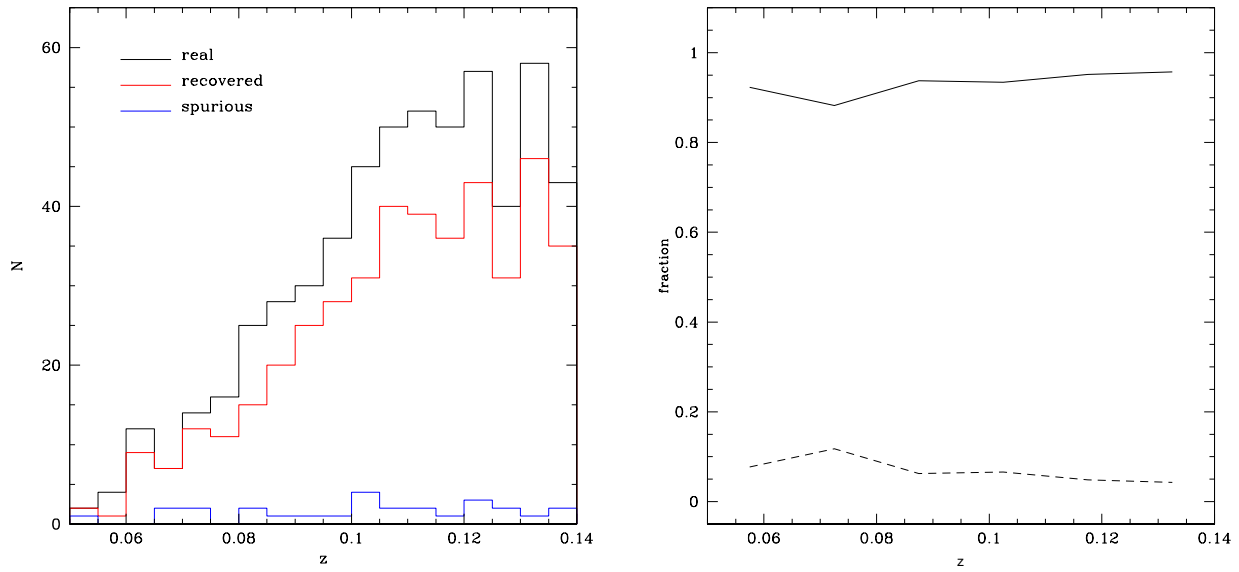


Figure 3. Completeness and contamination analysis. Left panel: Real, recovered and spurious systems redshift distributions. Right panel: Completeness (solid line) and contamination (dashed line) as function of redshift.

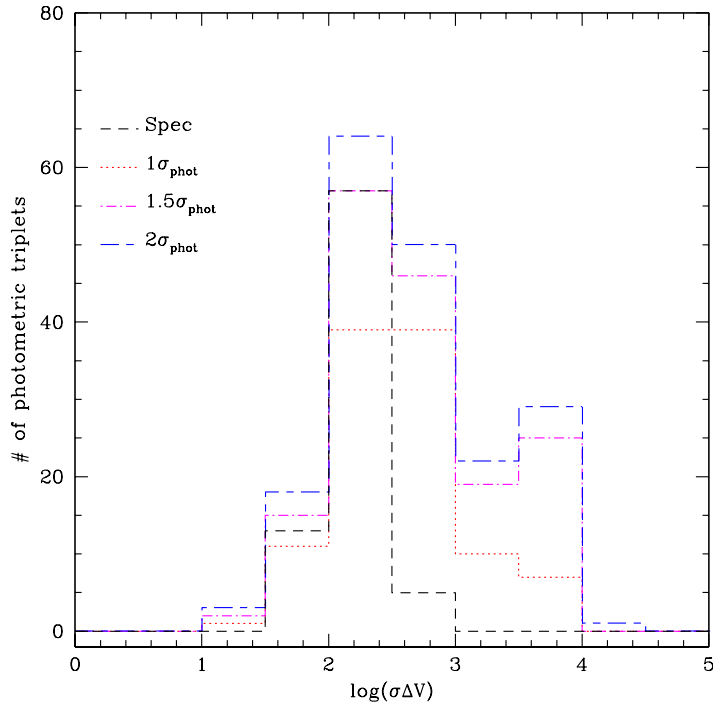


Figure 4. $\sigma_{\Delta V}$ spectroscopic distribution for photometric triplet candidates using S2 sample. Black (short dashed line): spectroscopic systems. Red (dotted), magenta (dot-short dashed line) and blue (short dashed-long dashed line): photometric systems obtained considering $1\sigma_{\text{phot}} * c$, $1.5\sigma_{\text{phot}} * c$ and $2\sigma_{\text{phot}} * c$ velocity intervals, respectively.

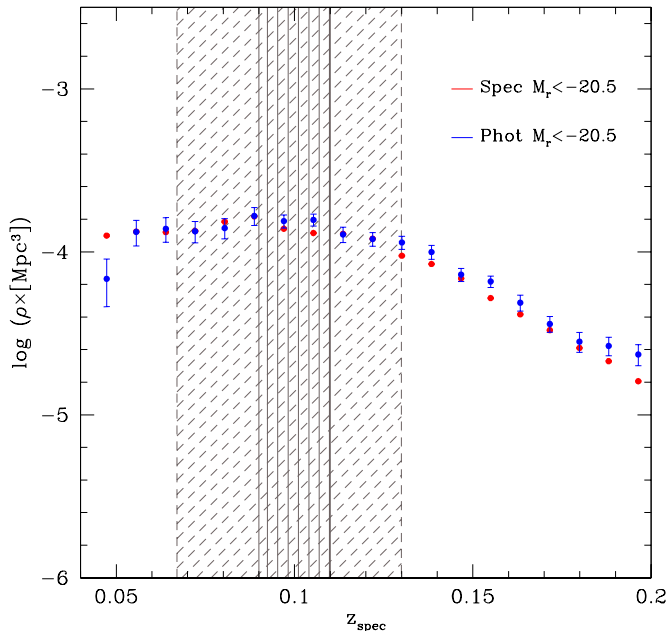


Figure 5. Spatial number density of galaxies as a function redshift for the MGS (red dots) and for a random sample with 0.001% of the photometric sample from O’Mill et al. (2011) (blue dots) both with $r < 17.77$. The error bars represent 1σ uncertainties calculated using bootstrap. For both samples the galaxy density for $z_{\text{spec}} < 0.14$ is nearly flat. The small and large regions correspond to redshift intervals employed in the analysis of fiber collision (S3 sample).

Zehavi et al. (2002) found that approximately 6% of the target objects are not assigned to a fiber due to the 55” restriction. Alonso et al. (2006) have identified pairs of galaxies in the MGS of SDSS second data release and analysed galaxy pairs loss due to fiber collision. These authors found that approximately 5% of the pairs were not recovered due to this effect. Recently Costa-Duarte et al. (2011) found that $\sim 40\%$ of galaxies with $r < 17.77$ have spectroscopic measurements.

In figure 5 we show the spatial galaxy density as a function of redshift for the MGS (red dots) and for a random sample with 0.001% of the photometric data from O’Mill et al. (2011) (blue dots) both with $r < 17.77$. It can be appreciated a nearly flat galaxy density for $z_{\text{spec}} < 0.14$. In order to evaluate the reliability of the identification procedure adopted in this work, we used the S3 sample considering spectroscopic and photometric triplets detected in the redshift range $0.09 \leq z_{\text{spec}} \leq 0.11$ (figure 5 small region) and $0.09 - \sigma_{\text{phot}} \leq z_{\text{phot}} \leq 0.11 + \sigma_{\text{phot}}$ (figure 5 large region) respectively. For a discussion about the uncertainties in the photometric redshift see subsection 4.3.

Using S3 sample we have obtained 64 triplet candidates with spectroscopic measurements. About $\sim 90\%$ of the systems had been recovered using photometric data. Nevertheless, there are 39 triplets with 1 or 2 members without spectroscopic information due to fiber collision. Figure 8 shows two examples of photometric triplet candidates where one or two galaxies do not have spectroscopic redshift determination.

We have taken into account these considerations and we have included these objects as triplet of galaxies candidates at low redshift.

5 IMPLEMENTATION OF THE ALGORITHM AT INTERMEDIATE REDSHIFT ($0.14 \leq z_{\text{phot}} \leq 0.4$)

From the discussion in Sections 4.3 and 4.4 we can see that photometric redshifts are suitable to identify triplet of bright galaxies candidates. The right panel of figure 1 show the galaxy density distribution as a function of redshift for the photometric S4 sample. It can be noticed the flat behaviour of the galaxy density up to $z_{\text{phot}} < 0.4$.

The uncertainty of the photometric redshifts became larger at low redshift (O’Mill et al. 2011). Taking into account these issues we assume a range $0.14 \leq z_{\text{phot}} \leq 0.4$ of reliability for the determination of photometric triplet candidates.

We run the algorithm for S4 sample considering the restrictions in ΔV according to the discussion of section 4.3.

Following the steps described in section 3.2, a total of 5628 triplet system candidates were obtained in the range $0.14 \leq z_{\text{phot}} \leq 0.4$, 3771 of them with the constraints $r_p < 100 h^{-1}$ kpc and $\Delta V < 6810 \text{ km s}^{-1}$ ($1\sigma_{\text{phot}} * c$) and 1857 with the second set of constrains $r_p < 200 h^{-1}$ kpc and $\Delta V < 9310 \text{ km s}^{-1}$ (corresponding to $\sim 1.37\sigma_{\text{phot}} * c$).

Figure 7 shows the distribution of the values of $\Delta V_{r.m.s}$ for the systems identified in the S4 sample, with the higher ΔV and r_p constraints (red line), as well as this distribution for systems identified relaxing these constraints (blue dashed line). From this figure it can be appreciated that both distributions show a similar behaviour.

6 ISOLATION CRITERIA

In the previous sections we have identified galaxy triplets candidates, regardless the relative spatial isolation of these systems. In order to build a catalogue of physical triplet systems, it is neces-

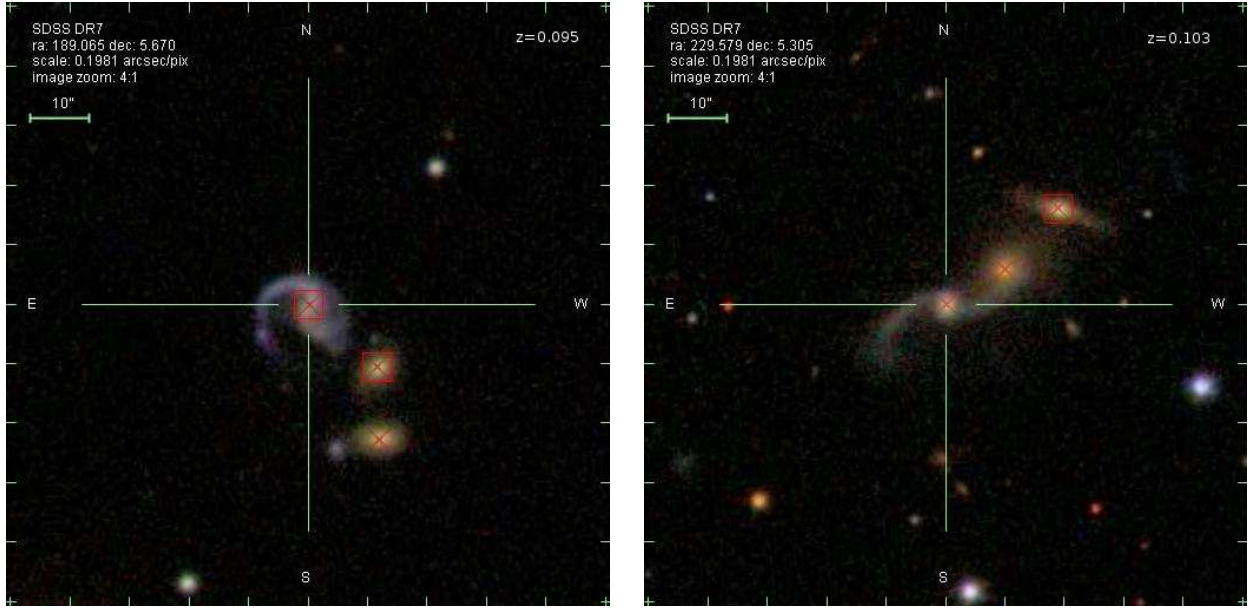


Figure 6. Examples of triplet candidates with photometric measurements obtained from S3 sample. Galaxies with redshift determination are marked with a box, and galaxies members are indicate with crosses.

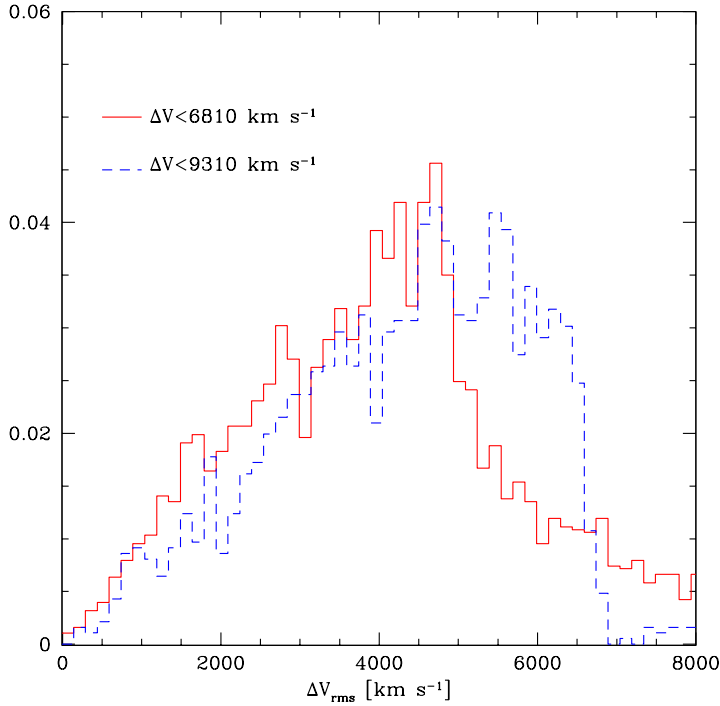


Figure 7. Distribution of ΔV_{rms} for the systems identified in S4 sample. Red line: $r_p < 100 h^{-1} \text{ kpc}$ and $\Delta V < 6810 \text{ km s}^{-1}$. Blue dashed line systems with $r_p < 200 h^{-1} \text{ kpc}$ and $\Delta V < 9310 \text{ km s}^{-1}$.

sary to define isolation criteria that ensures that the dynamics of these systems is not dominated by larger virialized structures where these systems could be immersed.

Physical triplets are a special case of a small group with three members. We have selected triplet candidates comprising luminous

galaxies. Nevertheless, from a dynamical point of view, there could be other neighbour galaxies with lower luminosity that affects the properties of the system.

Hereafter, we consider two proxies for galaxy environment:

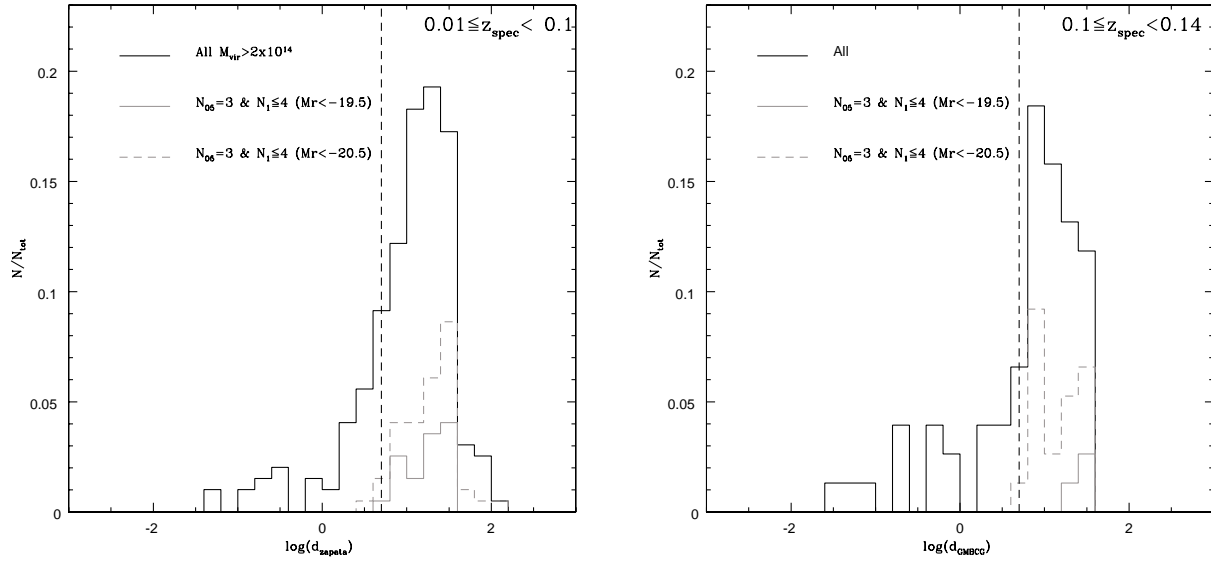


Figure 8. Distribution of the distance to the closest neighbour cluster for spectroscopic triplet candidates. Left panel: Distance to Zapata et al. (2009) for systems with $0.01 \leq z_{\text{spec}} < 0.1$. Right panel: Distance to GMBCG clusters for systems in the range with $0.1 \leq z_{\text{spec}} < 0.14$. Solid black line show the distribution of all the systems in that redshift range, in grey dashed line the distribution of the triplet candidates with $N05 = 3$ and $N1 \leq 4$ estimated using galaxies brighter than $M_r = -20.5$ and in solid grey line the systems with $N05 = 3$ and $N1 \leq 4$ estimated using galaxies brighter than $M_r = -19.5$. Vertical black dashed line show the $dc = 5 h^{-1} \text{Mpc}$ limit selected as part of the isolation criteria.

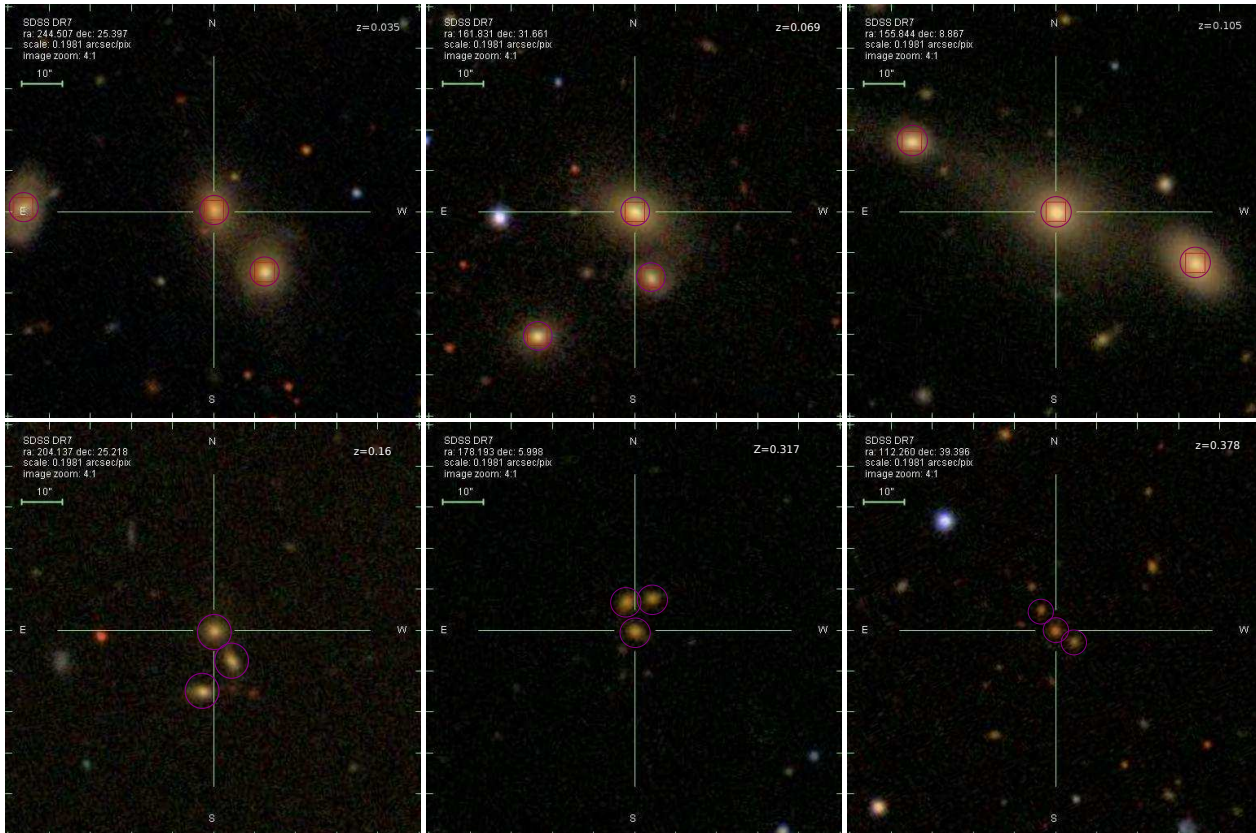


Figure 9. Examples of triplets with spectroscopic and photometric measurements in the redshift range $0.01 \leq z_{\text{phot}} \leq 0.4$. Galaxies with spectroscopy are marked with a box and triplet galaxies members with a circle.

one associated to the local environment, and another related to larger scales.

In order to describe global environment, we compute the distance to the closest neighbour cluster of galaxies. This quantity is related to the mass of the region where the galaxy resides (González & Padilla 2009). Nevertheless, even if a triplet candidate system is distant from high density regions, it could still be part of a larger group of galaxies. To avoid such systems we have employed a fixed aperture method to describe the local galaxy density.

Therefore, we have selected isolated triplets that satisfies the following criteria:

- (i) $N_{05} = 3$
- (ii) $N_1 \leq 4$
- (iii) $dc \geq 5 h^{-1}\text{Mpc}$

N_{05} and N_1 are the number of galaxies brighter than $M_r = -20.5$ within $0.5 h^{-1}\text{Mpc}$ and $1 h^{-1}\text{Mpc}$ respectively, with the same restrictions on ΔV used to identify triplet members, and dc is the distance to the closest neighbour cluster.

These criteria were chosen from an analysis of the triplet candidates at low redshifts ($0.01 \leq z < 0.14$) where we analysed the behaviour of N_{05} and N_1 for galaxies brighter than $M_r = -20.5$ and $M_r = -19.5$, in order to calibrate these two quantities for the selection of an isolation criterion to be applied at higher redshifts where only bright galaxies are included. In order to work with a complete sample of galaxies with a fainter limiting absolute magnitude than that given by the spectroscopic survey, we have considered galaxies brighter than $M_r = -19.5$ up to $z_{\text{spec}} = 0.14$, using both spectroscopic as well as photometric data. Accordingly, we estimate the N_{05} and N_1 parameter taking into account the photometric redshift errors.

In order to analyse the global environment we used the projected distance to the closest neighbour cluster in two cluster catalogues: we used a group/cluster sample extracted from the catalogue constructed by Zapata et al. (2009) updated to the SDSS-DR7 for $0.01 \leq z_{\text{spec}} < 0.1$ ($d_c = d_{\text{zapata}}$). For systems with $0.1 \leq z_{\text{spec}} < 0.14$ we have used the Gaussian Mixture Brightest Cluster Galaxy (GMBCG) catalogue (Hao et al. 2011) ($d_c = d_{\text{GMBCG}}$).

Zapata et al. (2009) employed a friends-of-friends algorithm with varying projected linking length σ , with $\sigma_0 = 0.239 h^{-1}\text{Mpc}$ and fixed radial linking length $\Delta V = 450\text{km s}^{-1}$. The sample comprises 15140 groups and extends out to $z = 0.12$. Following Padilla et al. (2010), we select groups with virial masses $M_{\text{vir}} > 10^{14} h^{-1} M_{\odot}$ and define a group/cluster sample. The GMBCG catalogue of clusters (Hao et al. 2011) comprises 55424 clusters identified using the red sequence plus Brightest Cluster Galaxy features, in the redshift range $0.1 \leq z < 0.55$. The cluster abundance of GMBCG clusters is similar to Zapata et al. (2009) provided a mass restriction $M_{\text{vir}} > 10^{14} h^{-1} M_{\odot}$ is applied to this sample.

Therefore, for each triplet system candidate we compute the projected distance to the closest neighbour cluster considering a radial velocity cut $\Delta V < 1000\text{km s}^{-1}$ when spectroscopic information is available and $\Delta V < 7000\text{km s}^{-1}$ for systems with photometric redshifts.

Figure 8 shows the distribution of the distance to the closest neighbour cluster (left Zapata et al. 2009 and right Hao et al. 2011), for the spectroscopic triplet candidates. In black solid line the distribution for systems in the redshift range $0.01 \leq z_{\text{spec}} < 0.1$ (left panel) and $0.1 \leq z_{\text{spec}} < 0.14$ (right panel). In these figures, grey dashed lines represent the distribution of triplet candidates that sat-

isfies $N_{05} = 3$ and $N_1 \leq 4$, estimated using galaxies brighter than $M_r = -20.5$. The distribution for systems with $N_{05} = 3$ and $N_1 \leq 4$, estimated with galaxies $M_r \leq -19.5$ is represented in grey solid line. In both panels of this figure it can be appreciated that the limit $dc = 5 h^{-1}\text{Mpc}$ (vertical black dashed line) encloses most of the systems with $N_{05} = 3$ and $N_1 \leq 4$ (galaxies $M_r \leq -19.5$ as well as galaxies with $M_r \leq -20.5$).

We have considered this limit in order to select a safe isolation criterion, for triplet candidates at higher redshift ($0.14 \leq z \leq 0.4$), where, by completeness, the selection of isolated triplets with $N_{05} = 3$ and $N_1 \leq 4$ can be estimated only by using galaxies brighter than $M_r = -20.5$.

Taking a distance greater than $5 h^{-1}\text{Mpc}$, we are ensuring that our triplets do not belong to any system of groups or clusters. On the other hand, by restricting the number of galaxies within $0.5 h^{-1}\text{Mpc}$ and $1 h^{-1}\text{Mpc}$ leave us with a system composed by only three luminous galaxies.

By imposing the isolation criterion to the sample of triplet of galaxies candidates we obtain 1092 triplets in our final catalogue, 95 triplets in the redshift range $0.01 \leq z_{\text{spec}} < 0.14$ and 997 in the range $0.14 \leq z_{\text{phot}} \leq 0.4$. Figure 9 shows three examples of the systems at low and intermediate redshifts. From these figures it can be appreciated the high degree of isolation of the systems. In a forthcoming paper (paper II, Duplancic et. al in preparation), we will analyse different spectro-photometric properties of these isolated triplet of galaxies systems.

In the Appendix we summarise some properties of 20 triplets from the final catalogue derived in this work. Columns 1 and 2 right ascension and declination (J2000) galaxy positions in hexadecimal format; column 3 redshift of the central galaxy, and column 4 number of triplet galaxy members with spectroscopic measurements. The full catalog is available electronically.

7 RESULTS AND DISCUSSION

In this work we have developed algorithms for the identification of galaxy triplet candidates in the Sloan Digital Sky Survey Data Release Seven.

Taking into account the completeness of the spectroscopic data in the range $0.01 \leq z_{\text{spec}} < 0.14$ down to absolute magnitude $M_r = -20.5$, we identified 273 triplet candidates using only the spectroscopic data.

We have considered the incompleteness of these spectroscopic triplets due to fiber collision by using photometric as well as spectroscopic data. We find that 90% of the spectroscopic systems can be recovered using the photometric data and, additionally, 39 new triplet candidates with 1 or 2 members without spectroscopic information were included into this sample.

In order to explore the completeness and contamination of our procedure, we have employed a mock catalogue with similar volume than the spectroscopic S1 sample. We find a high level of completeness ($\sim 80\%$) and low contamination ($\sim 5\%$) which gives confidence to the methods adopted and the results obtained.

Using photometric information we have extended the sample of triplet candidates in the spectroscopic redshift range up to significantly larger depths ($0.14 \leq z_{\text{phot}} \leq 0.4$). Within this larger redshift range we identified 5628 triple system candidates.

In order to build a catalogue of triplets of galaxies which fulfil the main features of physical systems, we defined an isolation criterion based on both, the distance to the closest neighbour cluster and a fixed aperture local density estimate. This criterion ensures

that the dynamics of the systems is not dominated by larger virialized structures and also avoids triplets contaminated by bright close neighbour galaxies.

By imposing the isolation criterion to the sample of triplet of galaxies candidates we obtain 1092 triplets in our final catalogue, 95 triplets in the redshift range $0.01 \leq z_{\text{spec}} < 0.14$ and 997 in the range $0.14 \leq z_{\text{phot}} \leq 0.4$. The results can be appreciated by inspection of Figure 10, which shows the spatial number density of isolated triplets as a function of redshift, for the low redshift sample. Red dots corresponds to the spectroscopic triplets and blue dots to the spatial number density with the new triplets included after the fiber collisions analysis (see section 4.4). From this figure it can be seen that photometric redshift information is useful in order to complete the sample of triplets at low redshift.

Figure 11 shows the spatial number density of isolated triplets as a function of redshift for the intermediate redshift sample. By comparison to figure 10 it can be appreciated that the spatial number density of both, the intermediate and the low redshift photometric triplet samples, smoothly match at $z \sim 0.14$. The observed flat behavior of the number density up to $z_{\text{phot}} \sim 0.4$ shows that our methods are adequate to identify triplets reliably without important systematic effects.

Our results show that photometric redshifts provide very useful information, allowing to asses fiber collision incompleteness and extend the detection of triplets to large distances where spectroscopic redshifts are not available.

The final catalogue comprise 1092 triplets of galaxies in the redshift range $0.01 \leq z \leq 0.4$. This sample is suitable for statistical analysis, which will be performed in a forthcoming paper, and may serve as targets for follow up observations.

8 ACKNOWLEDGEMENTS

We thank the authors Zapata, Perez, Padilla & Tissera for granting us access to their group catalogue. We thank the Referee for providing us with helpfull comments. This work was supported in part by the Consejo Nacional de Investigaciones Científicas y Técnicas de la República Argentina (CONICET), Secretaría de Ciencia y Tecnología de la Universidad de Córdoba and Secretaría de Ciencia y Técnica de la Universidad Nacional de San Juan. Ana Laura O'Mill and Laerte Sodr e Jr was supported by the Brazilian agencies FAPESP and CNPq. Funding for the SDSS and SDSS-II has been provided by the Alfred P. Sloan Foundation, the Participating Institutions, the National Science Foundation, the U.S. Department of Energy, the National Aeronautics and Space Administration, the Japanese Monbukagakusho, the Max Planck Society, and the Higher Education Funding Council for England. The SDSS Web Site is <http://www.sdss.org/>. The SDSS is managed by the Astrophysical Research Consortium for the Participating Institutions. The Participating Institutions are the American Museum of Natural History, Astrophysical Institute Potsdam, University of Basel, University of Cambridge, Case Western Reserve University, University of Chicago, Drexel University, Fermilab, the Institute for Advanced Study, the Japan Participation Group, Johns Hopkins University, the Joint Institute for Nuclear Astrophysics, the Kavli Institute for Particle Astrophysics and Cosmology, the Korean Scientist Group, the Chinese Academy of Sciences (LAMOST), Los Alamos National Laboratory, the Max-Planck-Institute for Astronomy (MPIA), the Max-Planck-Institute for Astrophysics (MPA), New Mexico State University, Ohio State University, University of Pittsburgh, University of Portsmouth, Princeton University, the

United States Naval Observatory, and the University of Washington.

REFERENCES

- Abazajian, K. N., et al. 2009, *ApJS*, 182, 543
 Aceves, H. 2000, *IAU Colloq. 174: Small Galaxy Groups*, 209, 286
 Agekyan, T. A., & Anosova, Z. P. 1967, *Astronomicheskii Zhurna*, 44, 1261
 Alonso, M. S., Tissera, P. B., Coldwell, G., & Lambas, D. G. 2004, *MNRAS*, 352, 1081
 Alonso, M. S., Lambas, D. G., Tissera, P., & Coldwell, G. 2006, *MNRAS*, 367, 1029
 Anosova, Z. P., Kiseleva, L. G., Orlov, V. V., & Chernin, A. D. 1992, *Sov. Astron.*, 36, 231
 Blanton, M. R., Lin, H., Lupton, R. H., Maley, F. M., Young, N., Zehavi, I., & Loveday, J. 2003, *AJ*, 125, 2276
 Blanton, M. R., & Roweis, S. 2007, *AJ*, 133, 734
 Chernin, A. D., & Mikkola, S. 1991, *MNRAS*, 253, 153
 Costa-Duarte, M. V. C., Sodr e, L., & Durrett, F. 2011, *MNRAS*, 411, 1716
 Croton, D. J., et al. 2006, *MNRAS*, 365, 11
 Domingue, D., & Xu, C. K. 2005, *Bulletin of the American Astronomical Society*, 37, 1455
 Ellison, S. L., Patton, D. R., Simard, L., & McConnachie, A. W. 2008, *AJ*, 135, 1877
 Elyiv, A., Melnyk, O., & Vavilova, I. 2009, *MNRAS*, 394, 1409
 Fukugita, M., Ichikawa, T., Gunn, J. E., Doi, M., Shimasaku, K., & Schneider, D. P. 1996, *AJ*, 111, 1748
 Geller, M. J., & Huchra, J. P. 1983, *ApJS*, 52, 61
 Gonz alez, R. E., & Padilla, N. D. 2009, *MNRAS*, 397, 1498
 G orski, K. M., Hivon, E., Banday, A. J., Wandelt, B. D., Hansen, F. K., Reinecke, M., & Bartelmann, M. 2005, *ApJ*, 622, 759
 Gunn, J. E., et al. 1998, *AJ*, 116, 3040
 Hao, J., Mckay, T., Koester, B., et al. 2011, *Bulletin of the American Astronomical Society*, 43, #213.06
 Hein am aki, P., Lehto, H. J., Valtonen, M. J., & Chernin, A. D. 1998, *MNRAS*, 298, 790
 Hern andez-Toledo, H. M., M endez-Hern andez, H., Aceves, H., & Olgu n, L. 2011, *AJ*, 141, 74
 Hogg, D. W., Blanton, M., & SDSS Collaboration 2001, *Bulletin of the American Astronomical Society*, 34, 570
 Karachentseva, V. E. 1973, *Astrofizicheskie Issledovaniia Izvestiya Spetsial'noj Astrofizicheskoy Observatorii*, 8, 3
 Karachentseva, V. E., Karachentsev, I. D., & Shcherbanovskii, A. L. 1979, *Astrofizicheskie Issledovaniia Izvestiya Spetsial'noj Astrofizicheskoy Observatorii*, 11, 3
 Karachentsev, I. D., & Karachentseva, V. E. 1981, *Astrofizika*, 17, 5
 Karachentseva, V. E., & Karachentsev, I. D. 1982, *Astrofizika*, 18, 5
 Karachentseva, V. E., & Karachentsev, I. D. 1983, *Astrofizika*, 19, 613
 Karachentsev, V. E., Karachentsev, I. D., & Lebedev, V. S. 1988, *Astrofizicheskie Issledovaniia Izvestiya Spetsial'noj Astrofizicheskoy Observatorii*, 26, 42
 Karachentsev, I. D., Karachentseva, V. E., & Lebedev, V. S. 1990, *NASA Conference Publication*, 3098, 115
 Karachentseva, V. E., & Karachentsev, I. D. 2000, *IAU Colloq. 174: Small Galaxy Groups*, 209, 11

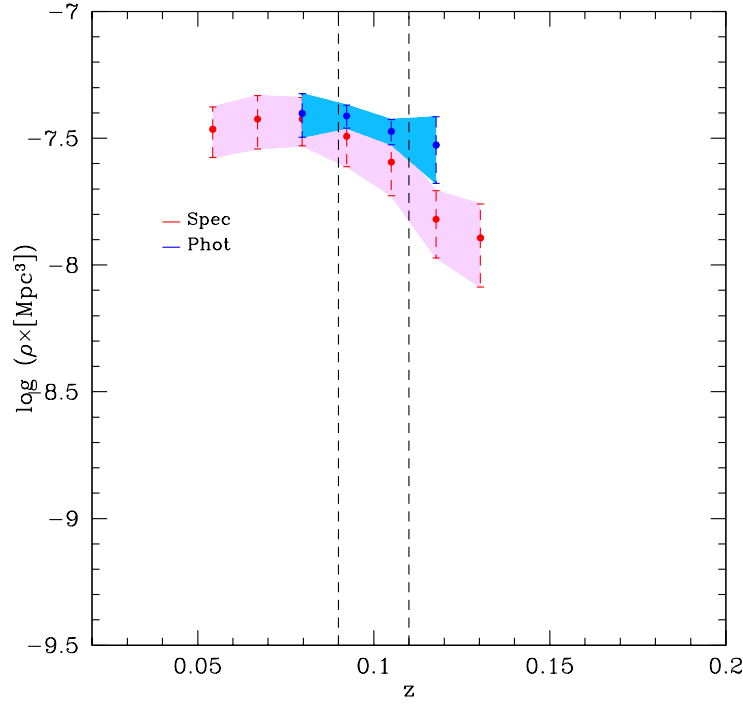


Figure 10. Spatial number density of isolated triplet of galaxy at low redshift. Red dots represents systems with spectroscopic information and in blue the spatial number density with the systems incorporated by using photometric information. The error bars represent 1σ uncertainties calculated using bootstrap techniques. Vertical lines shows the redshift range analysed in section 4.4.

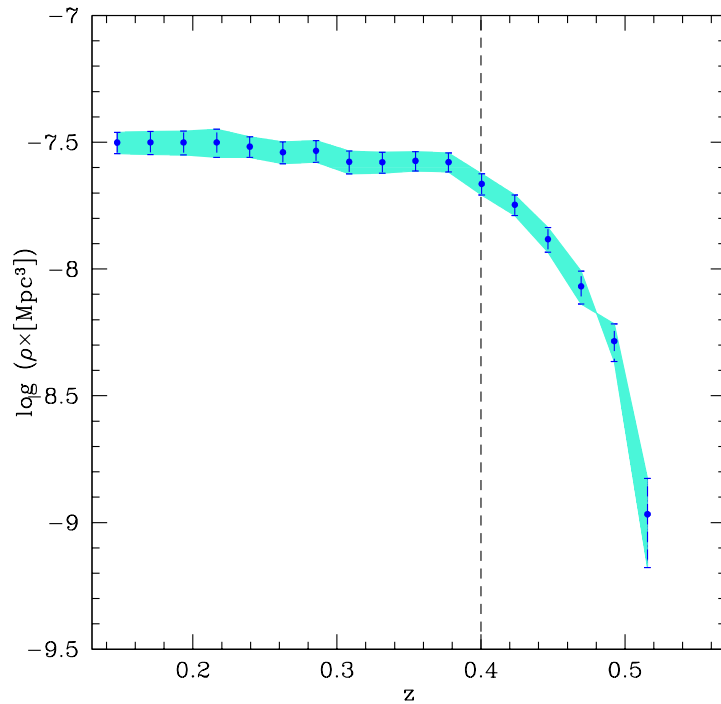


Figure 11. Spatial number density of isolated triplet of galaxy at intermediate redshift. The error bars represent 1σ uncertainties calculated using bootstrap techniques.

Lambas, D. G., Tissera, P. B., Alonso, M. S., & Coldwell, G. 2003, MNRAS, 346, 1189

Maia, M. A. G., da Costa, L. N., & Latham, D. W. 1989, ApJS, 69, 809

Merchán, M. E., & Zandivarez, A. 2005, ApJ, 630, 759

O’Mill, A. L., Duplancic, F, García Lambas, D., & Sodr e, L. 2010, MNRAS, in press.

Padilla, N., Lambas, D. G., & Gonz alez, R. 2010, MNRAS, 409, 936

Pier, J. R., Munn, J. A., Hindsley, R. B., Hennessy, G. S., Kent, S. M., Lupton, R. H., & Ivezi c,  . 2003, AJ, 125, 1559

Smith, J. A., Tucker, D. L., Allam, S. S., & Jorgensen, A. M. 2002, Bulletin of the American Astronomical Society, 34, 1272

Springel V., White S. D. M., Jenkins A., Frenk C. S., Yoshida N., Gao L., Navarro J., Thacker R., Croton D., Helly J., Peacock J. A., Cole S., Thomas P., Couchman H., Evrard A., Colberg J., Pearce F., 2005, Nature, 435, 629

Strauss, M. A., et al. 2002, AJ, 124, 1810

Trofimov, A. V., & Chernin, A. D. 1995, Astronomy Reports, 39, 308

Vavilova, I. B., Karachentseva, V. E., Makarov, D. I., & Melnyk, O. V. 2006, arXiv:astro-ph/0609622

Xin-Fa, D., Peng, J., Jun, S., Qun, Z., & Ji-Zhou, H. 2005, Astrophysical and Astrophysical Transactions, 24, 187

York, D. G., et al. 2000, AJ, 120, 1579

Zehavi, I., et al. 2002, ApJ, 571, 172

Zapata, T., Perez, J., Padilla, N., & Tissera, P. 2009, MNRAS, 394, 2229

Zheng, J.-Q., Valtonen, M. J., & Chernin, A. D. 1993, AJ, 105, 2047

Table A1. Examples of triplets of galaxies. Column 1 and 2: right ascension and declination galaxy position. Column 3: redshift of the central galaxy. Column 4: number of triplet galaxy members with spectroscopic measurements.

α ($J2000$)	δ ($J2000$)	redshift	# members with z_{spec}
07 29 02.43	39 23 45.76	0.378	0
07 29 07.89	45 17 25.93	0.240	1
09 53 27.44	49 00 30.45	0.347	0
10 07 50.36	00 31 54.62	0.093	1
10 23 22.62	08 52 01.11	0.105	3
10 47 19.52	31 39 38.56	0.069	3
12 14 31.24	08 22 25.71	0.074	3
12 34 29.58	32 53 37.44	0.108	3
12 36 15.72	05 40 13.24	0.095	2
13 36 32.90	25 13 05.15	0.146	0
13 37 24.89	41 11 10.15	0.389	0
14 01 43.37	21 37 21.52	0.332	0
14 04 05.64	08 10 09.85	0.262	0
14 04 20.47	08 38 54.09	0.302	0
14 07 10.10	64 50 40.58	0.269	0
14 43 28.41	13 11 43.88	0.133	3
15 16 45.33	07 10 33.34	0.104	1
15 18 18.93	05 18 17.95	0.103	1
15 26 45.25	18 44 32.07	0.088	3
16 18 00.75	25 23 35.13	0.036	3

APPENDIX A: CATALOGUE SUMMARISE

We present a short table (table A1) with some properties of 20 triplets from the final catalogue derived in this work.